Molecular, One- and Two-Dimensional Systems Built from Manganese(II) and Phthalate/Diimine Ligands: Syntheses, Crystal Structures and Magnetic Properties

Chengbing Ma,[a] Wenguo Wang,[a] Xiaofeng Zhang,[a] Changneng Chen,[a] Qiutian Liu,*[a] Hongping Zhu,[a] Daizheng Liao,[b] and Licun Li[b]

Keywords: Manganese / N ligands / Magnetic properties / Structure elucidation

Several new Mn^{II} compounds, $[Mn_2(Hphth)_2(phen)_4](Hphth)_2{\cdot}2H_2O$ (**1**; H_2phth = phthalic acid, phen = 1,10-phenanthroline), $[Mn_2(Hphth)_2(phen)_4](ClO_4)_2{\cdot}2H_2O$ (**2**), $[Mn_4(phth)_4(phen)_4(H_2O)_4]{\cdot}2EtOH$ (**3**), $\{[Mn_4(phth)_2(phen)_8](PF_6)_4\}_2$ (**4**), $[Mn_4(phth)_2(bipy)_8](ClO_4)_4{\cdot}2EtOH$ (**5**; bipy = 2,2′-bipyridine), $[Mn(phth)(bipy)(H_2O)_2]_n$ (**6**), and $[Mn(phth)(pyz)(H_2O)_2]_n$ (**7**; pyz = pyrazine), have been synthesized by treatment of the appropriate Mn^{2+} salt and H_2phth with different diimine ligands. They were characterized by X-ray diffraction and show a variety of nuclearities, ranging from dinuclear (**1** and **2**) to tetranuclear (**3**–**5**), and dimensionalities, ranging from a 1D chain (**6**) to a 2D layer network (**7**), in which the phthalates act as primary bridging ligands coordinating to Mn atoms through their carboxylate groups in various bonding modes. Variable-temperature magnetic susceptibility measurements reveal weak anti-ferromagnetic coupling interactions in **1**, **3**, **4** and **6**.

Introduction

There has been increasing interest in the study and synthesis of discrete polynuclear or low-dimensional systems of paramagnetic metal ions, driven to a large extent by their specific structural features, their promising application in diverse areas of technology, such as magnetic recording and magnetic optics in the field of molecular magnetism,[1,2] and their unique properties,[3] as well as their potential as model compounds for the study of the active sites of the metalloenzymes with interacting paramagnetic centers.[4–6] A commonly used strategy to obtain such systems is to select appropriate extended bridging ligands which can transmit magnetic interactions and bind several metal centers through various bonding modes. In this sense, the terephthalate ligand has been used in many synthetic systems, and has generated a great variety of complexes whose magnetic behaviors have been extensively studied.[7–17] However, phthalate, an *o*-isomer of terephthalate, has been used only sparingly for this purpose,[18–20] in spite of the fact that it exhibits versatile bonding modes in metal complexes,[21] and that the neighboring carboxyls are noncoplanar with themselves and with the benzene ring. This could make the phthalate a promising candidate to produce new cluster topologies and to transmit various magnetic interactions.

Special attention has been paid to the structure and properties of manganese carboxylate cluster complexes due to their biological significance.[4,5,22] The Mn^{2+} ion usually plays a structural and/or hydrolytic role;[23] it is also found in some redox enzymes in the reduced form. Dinuclear manganese centers exist in manganese catalase, catalytically disproportionating H_2O_2,[24] and in ribonucleotide reductase, facilitating the reduction of RNA to DNA.[25] A tetranuclear manganese cluster in the oxygen-evolving center (OEC) of photosystem II successfully oxidizes H_2O to O_2,[26,27] though its structure is still a mystery. Recently, it has been shown that one pyrophosphatase needs three Mn^{2+} ions for catalytic activity.[28] To date, the chemistry of manganese cluster complexes with simple acetate and benzoate ligands has been fully developed,[29] but the use of dicarboxylate ligands for this purpose is relatively uncommon.[30–32] In the course of our ongoing work on manganese complexation by dicarboxylates, we have reported a trivalent dinuclear manganese complex with a (μ-oxo)bis(μ-Hphth) bridging core,[33] and have explored the structural transformation mediated by *o*-, *m*- and *p*-phthalate.[34] In this paper, keeping in mind that the number of the manganese complexes derived from phthalate is still low,[31,33–37] we have further explored the reaction of phthalic acid and a manganese(II) salt, with the introduc-

[a] State Key Laboratory of Structural Chemistry, Fujian Institute of Research on the Structure of Matter, Chinese Academy of Sciences,
Fuzhou 350002, China
Fax: (internat.) +86-591-3714946
E-mail: lqt@ms.fjirsm.ac.cn
[b] Department of Chemistry, Nankai University,
Tianjin 300071, China

Supporting information for this article is available on the WWW under http://www.eurjic.org or from the author.

  DOI: 10.1002/ejic.200400166

tion of the chelating 2,2′-bipyridine (bipy) and 1,10-phenanthroline (phen) ligands and the *exo*-bidentate μ-pyrazine (pyz) ligand as ancillary ligands, with the aim of inhibiting the expansion of the polymeric frameworks in order to obtain the desired polynuclear and low-dimensional complexes, or to induce the evolution of a novel structure, and obtained a new series of compounds (**1**−**7**). Various coordination modes of the phthalate to the Mn ion (Scheme 1) and a wide variety of structural topologies for these complexes are found. The magnetic properties of selected compounds are also discussed.

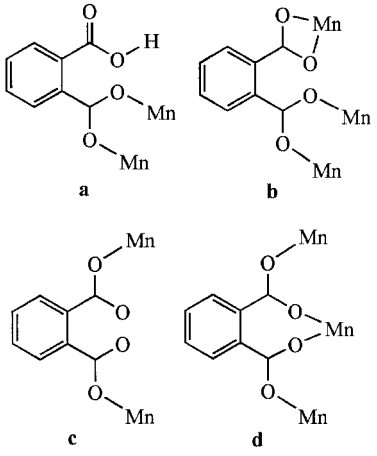

Scheme 1. Coordination modes of phthalate: (a) mono-bidentate; (b) bridging and chelating bis-bidentate; (c) bis-monodentate; (d) chelating/bridging bis-bidentate

Results and Discussion

Synthesis

Treatment of a mixture of H_2phth and an Mn^{2+} salt in the presence of various diimines gave compounds **1**−**7**, which were successfully isolated under different crystallization conditions. Partial deprotonation of H_2phth (H_2phth/KOH = 1:1) avoids the immediate precipitate derived from the direct reaction of $phth^{2-}$, Mn^{2+} and phen in EtOH/H_2O, leading to the formation of dinuclear compounds **1** and **2** with double μ-Hphth bridges; the use of H_2phth in the absence of KOH gave a known inclusion complex $[Mn(phen)_2(H_2O)Cl]Cl·0.5H_2phth$.[38] In general, increasing the KOH/H_2phth molar ratio is favorable to the complete deprotonation of H_2phth and leads to Mn complexes **3**, **4**, **6** and **7** containing completely deprotonated phthalate. Complex **5** contains a partially deprotonated Hphth ligand, probably due to the higher basicity of bipy. The use of neutral H_2phth and bipy resulted in the formation of a known Hphth compound with an $[Mn_2(\mu\text{-}O)(\mu\text{-}Hphth)_2]$ core.[33] The cyclic tetramanganese cluster **5** was isolated in the presence of bipy, while under similar conditions we only isolated the dinuclear complex **2** in the presence of phen. However, refluxing the reaction mixture containing $phth^{2-}$, Mn^{2+} and phen in EtOH/H_2O for several days caused the above-mentioned precipitate to dissolve, and led to the serendipitous formation of **3** and **4** from a one-pot reaction process. Here, PF_6^- as a specific counterion is crucial for the crystallization of both the compounds, even though there is no PF_6^- in compound **3**. When other counterions such as ClO_4^- was used instead of PF_6^-, we only isolated compound **2**. We also tried to omit the counterion from the reaction system, but either compound **1** or a known polymeric compound $[Mn(phth)(phen)(H_2O)_2]_n$ [35] was obtained depending on the degree of deprotonation of H_2phth. Attempts to prepare a bipy complex structurally analogous to **3** failed, even when varying counterion, solvent and starting Mn^{2+} salt. As expected, complex **7**, with a 2D layer framework, was isolated when the *exo*-bidentate μ-pyz ligand was used as the secondary linker instead of the chelating bipy ligand, as it is the end-capping bipy ligand that blocks the way towards higher dimensionality and maintains the 1D chain-like structure of **6**.

Structure Descriptions of Complexes 1−7

Both **1** and **2** contain the $[Mn_2(Hphth)_2(phen)_4]^{2+}$ cation, counterions and solvate water molecules in a molar ratio of 1:2:2 in the unit cell. The cations in **1** and **2** possess similar structural parameters, as listed in Table 1. Two equivalent Mn atoms related by a crystallographic inversion center are bridged by two carboxylate groups of Hphth ligands (Figure 1) in a *syn-anti* mode. The metal−metal distance of 4.786 Å for **1** (4.836 Å for **2**) is the largest amongst analogous dinuclear Mn^{2+} complexes with only two *syn-anti* bridging carboxylate groups: $[Mn_2(PhCOO)_2(bipy)_4]^{2+}$ (4.509 Å),[39] $[Mn_2(MeCOO)_2(bipy)_4]^{2+}$ (4.583 Å)[40] and $[Mn_2(ClCH_2COO)_2(phen)_4]^{2+}$ (4.613 Å).[41] The Mn atom

Table 1. Selected bond lengths (Å) and angles (°) for **1** and **2**

	Complex **1**	Complex **2**
Mn−O1	2.1176(16)	2.117(2)
Mn−O2A	2.1342(14)	2.127(2)
Mn−N3	2.2557(19)	2.260(3)
Mn−N2	2.265(2)	2.247(3)
Mn−N1	2.269(2)	2.271(3)
Mn−N4	2.3088(18)	2.286(3)
O1−Mn−O2A[a]	94.71(6)	92.94(9)
O1−Mn−N3	92.24(7)	92.14(10)
O2A−Mn−N3	89.56(6)	89.59(10)
O1−Mn−N2	97.32(8)	96.20(11)
O2A−Mn−N2	101.32(7)	100.50(11)
N2−Mn−N3	164.82(7)	166.53(11)
O1−Mn−N1	169.50(7)	168.65(12)
O2A−Mn−N1	92.25(6)	93.71(10)
N3−Mn−N1	95.67(8)	97.10(11)
N2−Mn−N1	73.57(8)	73.54(12)
O1−Mn−N4	85.42(6)	83.45(10)
O2A−Mn−N4	162.77(7)	162.50(10)
N3−Mn−N4	73.23(7)	73.50(11)
N2−Mn−N4	95.73(7)	96.92(11)
N1−Mn−N4	90.25(7)	92.83(10)

[a] Symmetry codes: (**1**) A: $-x, -y + 1, -z + 2$; (**2**) A: $-x + 2, -y + 2, -z$.

is in a distorted octahedral geometry, coordinated by four N atoms [Mn−N = 2.2557(19)−2.3088(18) Å for **1**, and 2.247(3)−2.286(3) Å for **2**] from two chelating phen ligands and two O atoms [Mn−O = 2.1176(16) Å and 2.1342(14) Å for **1**, and 2.117(2) Å and 2.127(2) Å for **2**] from bridging carboxylate groups. The Hphth, which acts as a mono-bidentate ligand (see a in Scheme 1), employs just one μ_2-carboxylate group to bridge two Mn atoms, with the other protonated one free. The characteristic IR absorptions for the stretching vibration of the protonated carboxylic group of Hphth appear at 1689 cm^{-1} for **1** (1701 cm^{-1} for **2**). The bond-valence sum (BVS) calculations based on the equation $s = \exp[(r_0 - r)/B]$[42] (r is the observed bond length and r_0 and B are empirically determined parameters[43]) give values of 1.97 and 1.99 for **1** and **2**, respectively, indicating that the Mn centers in both compounds are in the +2 oxidation state, and that the ligand is a partially deprotonated phthalate anion. The other complexes in this work gave similar values and are therefore not discussed further.

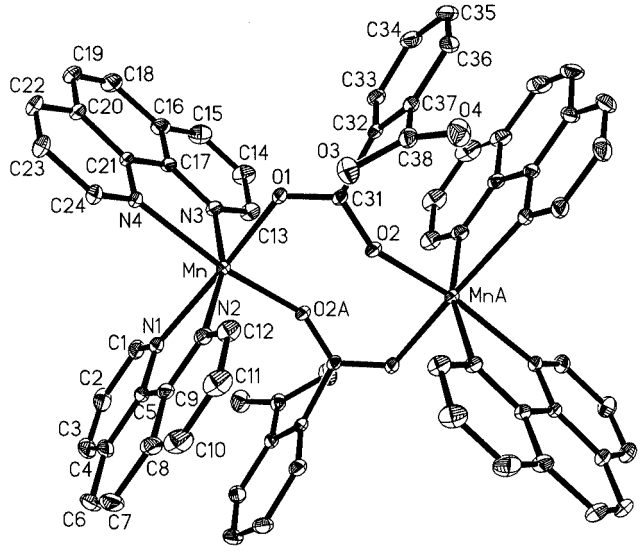

Figure 1. The structural view of the cation in **1** and **2** (ellipsoids at 20% probability)

Some differences were observed between the hydrogen-bonding networks of compounds **1** and **2**. Besides a short intramolecular hydrogen bond with an O6···O7 distance of 2.376 Å found in the uncoordinated Hphth ions, three intermolecular hydrogen bonds also exist in the structure of **1**. The water molecule (O9) bridges the coordinated Hphth ions of the adjacent cations through two hydrogen bonds to produce 1D chains [O9···O4$^{\#}$ 2.763 Å; O3···O9$^{\&}$ 2.544 Å; &: $-x - 1, -y + 1, -z + 1$; #: $x, y, z - 1$] (see a in Figure 2); the uncoordinated Hphth ions link to the hydrogen-bonded chain through a third intermolecular hydrogen bond with an O9···O8 distance of 2.725 Å. As for compound **2**, besides a hydrogen bond between the solvate water molecules, with an O9···O9 distance of 2.502 Å, a second intermolecular hydrogen bond between the protonated carboxylic groups of the adjacent cations links together the cations of **2** to form 1D hydrogen-bonded chains [O3···O4$^{\#}$ 2.634 Å; #: $-x + 3, -y + 2, -z$] (see b in Figure 2); no hydrogen-bonding interaction with the ClO_4^- counterion was observed.

The crystal structure of **3** contains one neutral discrete tetramanganese cluster and two solvate ethanol molecules in each independent crystallographic unit. The whole molecule lies on a crystallographic inversion center implying that only two Mn atoms (Mn1 and Mn2) are crystallographically independent. As shown in Figure 3, the four coplanar Mn^{2+} ions arrayed at the four corners of an approximate rhombus (sides 6.069−6.301Å and angles 140.65° and

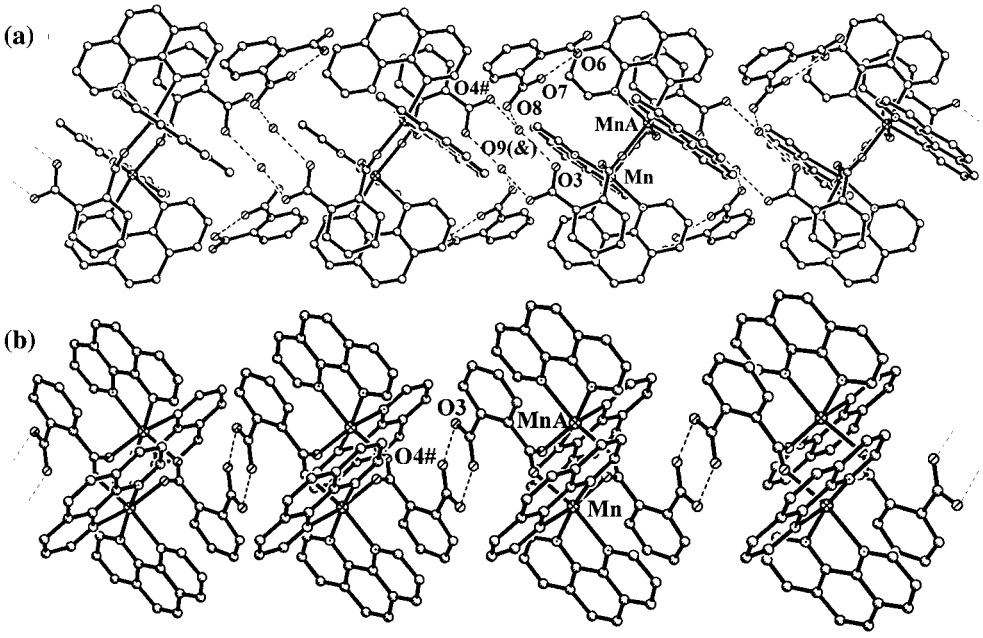

Figure 2. A view of the 1D hydrogen-bonded chains in **1** (a), and **2** (b)

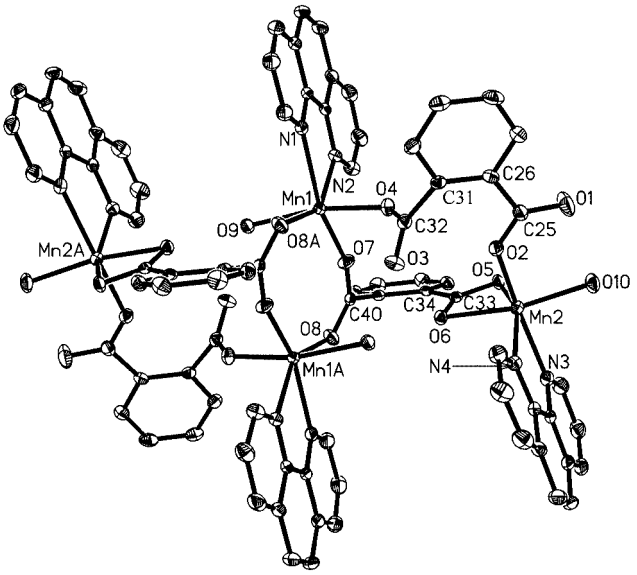

Figure 3. The structural view of the neutral tetranuclear cluster in **3** (ellipsoids at 30% probability)

39.35°), are bridged by two symmetry-related μ_3-phth ligands, one above and one below the Mn_4 rhombic plane. It is noteworthy that the phth ligand displays a unique bridging and chelating bis-bidentate mode, coordinating to three metal atoms through its one bridging carboxylate group and one chelating carboxylate group (see b in Scheme 1). To the best of our knowledge, this type of coordination mode for the phth ligand has not been found in other metal complexes.[21] In the Mn_4 rhombus, the two central Mn atoms (Mn1 and Mn1A, Mn1···Mn1A = 4.170 Å) are bridged by two bridging carboxylate groups of μ_3-phth ligands, and further linked to the two outer Mn atoms (Mn2 and Mn2A) through another chelating end of the same μ_3-phth ligands. Two bis-monodentate μ_2-phth ligands (see c in Scheme 1), four chelating phen ligands and four terminal water ligands complete the peripheral ligation, meaning that the Mn centers have distorted octahedral geometries (Table 2). All the phen-ring planes are nearly parallel with each other.

Table 2. Selected bond bengths (Å) and angles (°) in **3**

Mn1−O7	2.106(2)	O9−Mn1−N2	90.46(9)
Mn1−O4	2.110(2)	O7−Mn1−N1	156.93(10)
Mn1−O8A[a]	2.139(2)	O4−Mn1−N1	91.11(9)
Mn1−O9	2.289(2)	O8A−Mn1−N1	80.18(9)
Mn1−N2	2.324(3)	O9−Mn1−N1	97.64(9)
Mn1−N1	2.359(3)	N2−Mn1−N1	70.43(9)
Mn2−O2	2.099(2)	O2−Mn2−O10	87.32(10)
Mn2−O10	2.155(3)	O2−Mn2−O5	102.86(9)
Mn2−O5	2.200(2)	O10−Mn2−O5	102.97(10)
Mn2−N4	2.218(3)	O2−Mn2−N4	92.84(10)
Mn2−N3	2.287(3)	O10−Mn2−N4	98.97(11)
Mn2−O6	2.323(2)	O5−Mn2−N4	153.45(9)
O7−Mn1−O4	89.81(9)	O2−Mn2−N3	165.12(10)
O7−Mn1−O8A	122.84(9)	O10−Mn2−N3	88.09(11)
O4−Mn1−O8A	91.47(9)	O5−Mn2−N3	91.96(9)
O7−Mn1−O9	85.49(9)	N4−Mn2−N3	73.91(10)
O4−Mn1−O9	167.77(9)	O2−Mn2−O6	94.24(8)
O8A−Mn1−O9	81.67(9)	O10−Mn2−O6	160.57(10)
O7−Mn1−N2	86.75(9)	O5−Mn2−O6	57.78(7)
O4−Mn1−N2	100.57(9)	N4−Mn2−O6	100.29(9)
O8A−Mn1−N2	148.28(9)	N3−Mn2−O6	94.79(9)

[a] Symmetry code: A: $-x + 1, -y + 1, -z + 1$.

It is worth noting that the rhombic Mn_4 cluster in **3**, with an unprecedented [$Mn_4(\mu_3$-phth$)_2$] core, provides an important addition to the available Mn_4 aggregate database, although several rhombic or "butterfly-like" Mn_4 carboxylate clusters with an [Mn_4{μ-carboxilic-O(H)}] core have been reported.[29,44−49]

Some interesting supramolecular contacts are observed in the solid-state structure of **3**. One hydrogen bond links the coordinated water molecule (O10) and the carboxyl O atom (O5) of the symmetry-related Mn-tetramer to generate 1D hydrogen-bonded ribbons [O10···O5& 2.723 Å; &:

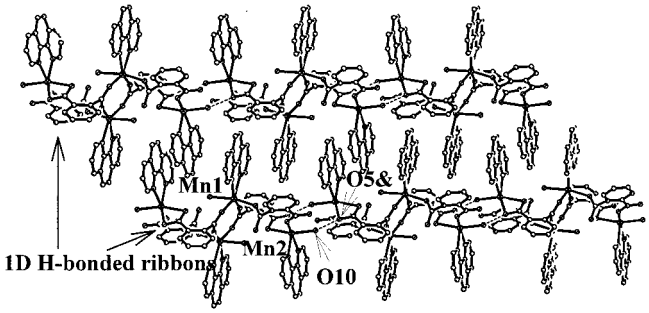

Figure 4. A view of the 2D supramolecular layer in **3**, showing the zipper-like intercalation of adjacent 1D hydrogen-bonded ribbons through face-to-face π-π interactions between the phen ligands; only two 1D hydrogen-bonded ribbons are displayed for clarity

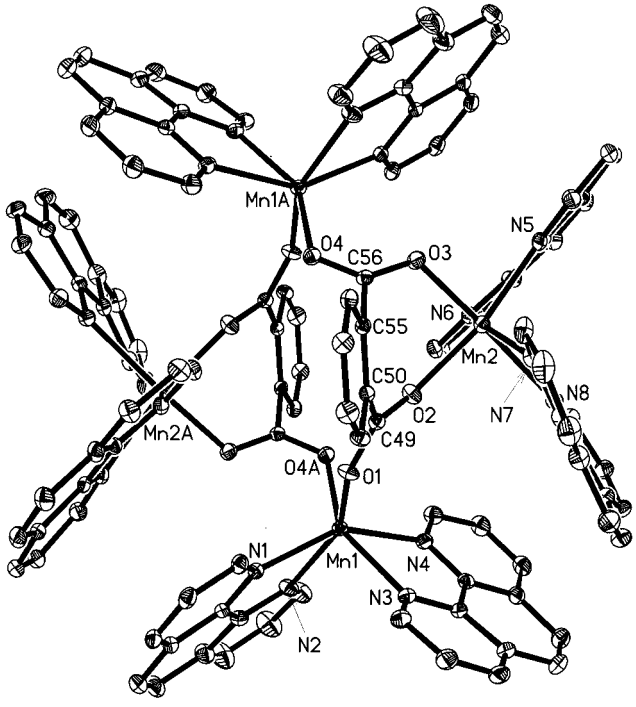

Figure 5. The structural view of one of the tetranuclear cluster cations in **4** (ellipsoids at 20% probability)

$-x, -y, -z$]; the adjacent ribbons are further intercalated in a zipper fashion into a 2D supramolecular layer through inter-ribbon π-π stacking interactions between the phen ligands, with face-to-face distances of 3.212−3.338 Å (Figure 4).

Each independent crystallographic unit of **4** contains two distinct, but very similar, discrete tetramanganese cluster cations, $[Mn_4(phth)_2(phen)_8]^{4+}$, and eight PF_6^- anions. The structure of one of these cations is shown in Figure 5. The cation possesses a crystallographically imposed center of symmetry implying that only two Mn atoms (Mn1 and Mn2) are crystallographically independent. The four coplanar Mn^{2+} ions are singly bridged by four *syn-anti* carboxylate groups from two phth ligands, each of which adopts a chelating/bridging bis-bidentate mode (Scheme 1d) to coordinate to three Mn atoms, forming a 16-membered nonplanar macrocyclic structure $(-Mn-O-C-O)_4$, with four Mn atoms located at the four corners of an approximate molecular rectangle of sides 4.941 Å and 5.456 Å. Each Mn center exhibits a strongly distorted octahedral geometry (Table 3), being coordinated by four N atoms [Mn−N = 2.288(5)−2.317(5) Å for Mn1; 2.222(5)−2.336(5) Å for Mn2] of two chelating phen ligands, and two O atoms [Mn−O = 2.100(4) Å for Mn1; 2.110(4) Å for Mn2] of carboxylate groups of phth ligand (s). The difference between the coordination environments around Mn1 and Mn2 is that the two O atoms coordinated to Mn1 belong to two phth ligands, whereas the two O atoms coordinated to Mn2 are from two ends of one phth ligand. There are no close intermolecular contacts in the structure, and the tetramanganese cluster units are well isolated, with a shortest intermolecular Mn···Mn distance of 8.573 Å.

Table 3. Selected bond lengths (Å) and angles (°) in **4** and **5**

Complex **4**			
Mn1−O1	2.100(4)	N3−Mn1−N4	71.13(19)
Mn1−O4A[a]	2.100(4)	N2−Mn1−N4	88.89(19)
Mn1−N1	2.288(5)	O3−Mn2−O2	87.78(17)
Mn1−N3	2.301(5)	O3−Mn2−N6	105.20(17)
Mn1−N2	2.306(5)	O2−Mn2−N6	91.14(17)
Mn1−N4	2.317(5)	O3−Mn2−N7	97.79(19)
Mn2−O3	2.110(4)	O2−Mn2−N7	94.24(18)
Mn2−O2	2.110(4)	N6−Mn2−N7	156.57(18)
Mn2−N6	2.222(5)	O3−Mn2−N5	88.61(16)
Mn2−N7	2.242(5)	O2−Mn2−N5	163.39(17)
Mn2−N5	2.250(5)	N6−Mn2−N5	74.19(18)
Mn2−N8	2.336(5)	N7−Mn2−N5	102.32(19)
O1−Mn1−O4A	94.97(16)	O3−Mn2−N8	169.53(17)
O1−Mn1−N1	84.30(17)	O2−Mn2−N8	89.62(17)
O4A−Mn1−N1	118.59(16)	N6−Mn2−N8	84.99(17)
O1−Mn1−N3	84.18(18)	N7−Mn2−N8	72.28(18)
O4A−Mn1−N3	149.89(17)	N5−Mn2−N8	96.67(17)
N1−Mn1−N3	91.34(17)	N1−Mn1−N4	149.63(17)
O1−Mn1−N2	154.08(19)	N3−Mn1−N4	71.13(19)
O4A−Mn1−N2	88.27(18)	N2−Mn1−N4	88.89(19)
N1−Mn1−N2	71.71(18)	O3−Mn2−O2	87.78(17)
N3−Mn1−N2	105.52(19)	O3−Mn2−N6	105.20(17)
O1−Mn1−N4	117.03(18)	O2−Mn2−N6	91.14(17)
O4A−Mn1−N4	82.77(17)	O3−Mn2−N7	97.79(19)
N1−Mn1−N4	149.63(17)	O2−Mn2−N7	94.24(18)
Complex **5**			
Mn1−O1	2.101(3)	N2−Mn1−N1	71.50(15)
Mn1−O4A[a]	2.113(3)	O1−Mn1−N4	85.83(12)
Mn1−N3	2.262(4)	O4A−Mn1−N4	158.02(13)
Mn1−N2	2.271(4)	N3−Mn1−N4	71.09(12)
Mn1−N1	2.305(4)	N2−Mn1−N4	97.72(13)
Mn1−N4	2.393(3)	N1−Mn1−N4	85.20(13)
Mn2−O2	2.127(3)	O2−Mn2−O3	84.67(12)
Mn2−O3	2.159(3)	O2−Mn2−N8	99.54(13)
Mn2−N8	2.230(3)	O3−Mn2−N8	89.74(12)
Mn2−N7	2.248(4)	O2−Mn2−N7	99.31(13)
Mn2−N5	2.266(3)	O3−Mn2−N7	162.44(12)
Mn2−N6	2.276(4)	N8−Mn2−N7	72.75(13)
O1−Mn1−O4A	97.52(12)	O2−Mn2−N5	91.49(13)
O1−Mn1−N3	107.58(12)	O3−Mn2−N5	101.87(12)
O4A−Mn1−N3	87.27(12)	N8−Mn2−N5	164.71(14)
O1−Mn1−N2	155.93(15)	N7−Mn2−N5	95.14(13)
O4A−Mn1−N2	88.05(14)	O2−Mn2−N6	156.63(13)
N3−Mn1−N2	96.03(14)	O3−Mn2−N6	83.26(13)
O1−Mn1−N1	85.17(14)	N8−Mn2−N6	100.33(14)
O4A−Mn1−N1	116.67(13)	N7−Mn2−N6	98.22(14)
N3−Mn1−N1	151.71(14)	N5−Mn2−N6	71.62(14)

[a] Symmetry code: A: $-x + 1, -y + 1, -z + 1$.

In each independent crystallographic unit of **5**, there is one discrete tetramanganese cluster cation, $[Mn_4(phth)_2(bipy)_8]^{4+}$, four ClO_4^- anions and two solvate ethanol molecules. The composition of the cation is similar to that in **4**, except that the chelating ligand is bipy in **5** rather than phen. In the structure of the cation (Figure 6), the phth ligand adopts the same coordination mode to that found in **4**, and the four Mn^{2+} ions also form a cyclic structure. Similarly to those found in **4**, the coordination environments around Mn1 and Mn2 are strongly distorted octahedral (Table 3), with four N atoms [Mn−N = 2.262(4)−2.393(3) Å for Mn1; 2.230(3)−2.276(4) Å for Mn2] of two chelating bipy ligands and two O atoms

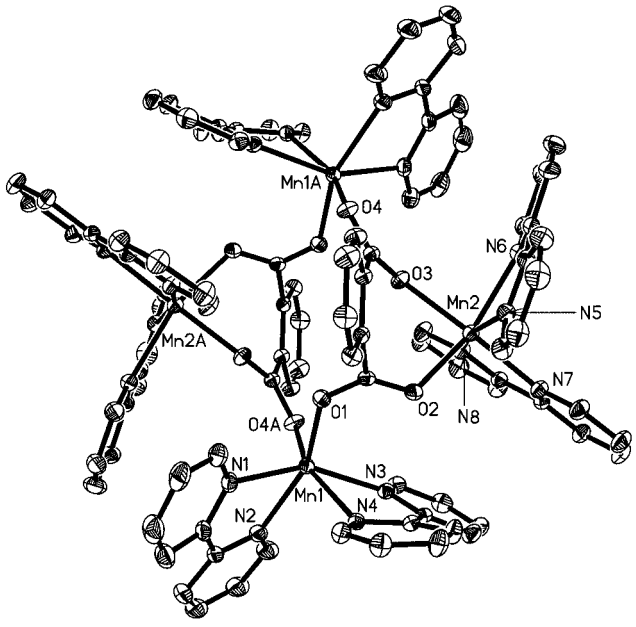

Figure 6. The structural view of the tetranuclear cluster cation in **5** (ellipsoids at 20% probability); Mn···Mn2A = 5.199 Å and Mn···Mn2 = 5.416 Å

[Mn−O = 2.101(3) and 2.113(3) Å for Mn1; 2.127(3) and 2.159(3) Å for Mn2] of carboxylate groups of the phth ligand (s) at the six apexes of the Mn octahedron. A similar complex with the same cationic core has been reported previously.[31]

Compound **6** consists of infinite 1D chains in which adjacent Mn atoms, with an interatomic distance of 7.131 Å, are bridged by one phth ligand (Figure 7a). The Mn atom is in a distorted octahedral geometry (Table 4), being coordinated by two N atoms [Mn−N1 = 2.312(2) Å, Mn−N2 = 2.289(2) Å] of one chelating bipy ligand, two O atoms [Mn−O5 = 2.193(2) Å, Mn−O6 = 2.285(2) Å] of water molecules and two O atoms [Mn−O1 = 2.128(2) Å, Mn−O4A = 2.135(2) Å] from bis-monodentate phth ligands (Scheme 1c). All bipy ligands parallel to each other are located on one side of the chain, with a dihedral angle of 105.4° between the bipy ligand plane and the benzene ring plane of the phth ligand, forming an unsymmetric chain structure. It should be noted that the coordination mode for the phth ligand exhibited in **6** differs greatly from

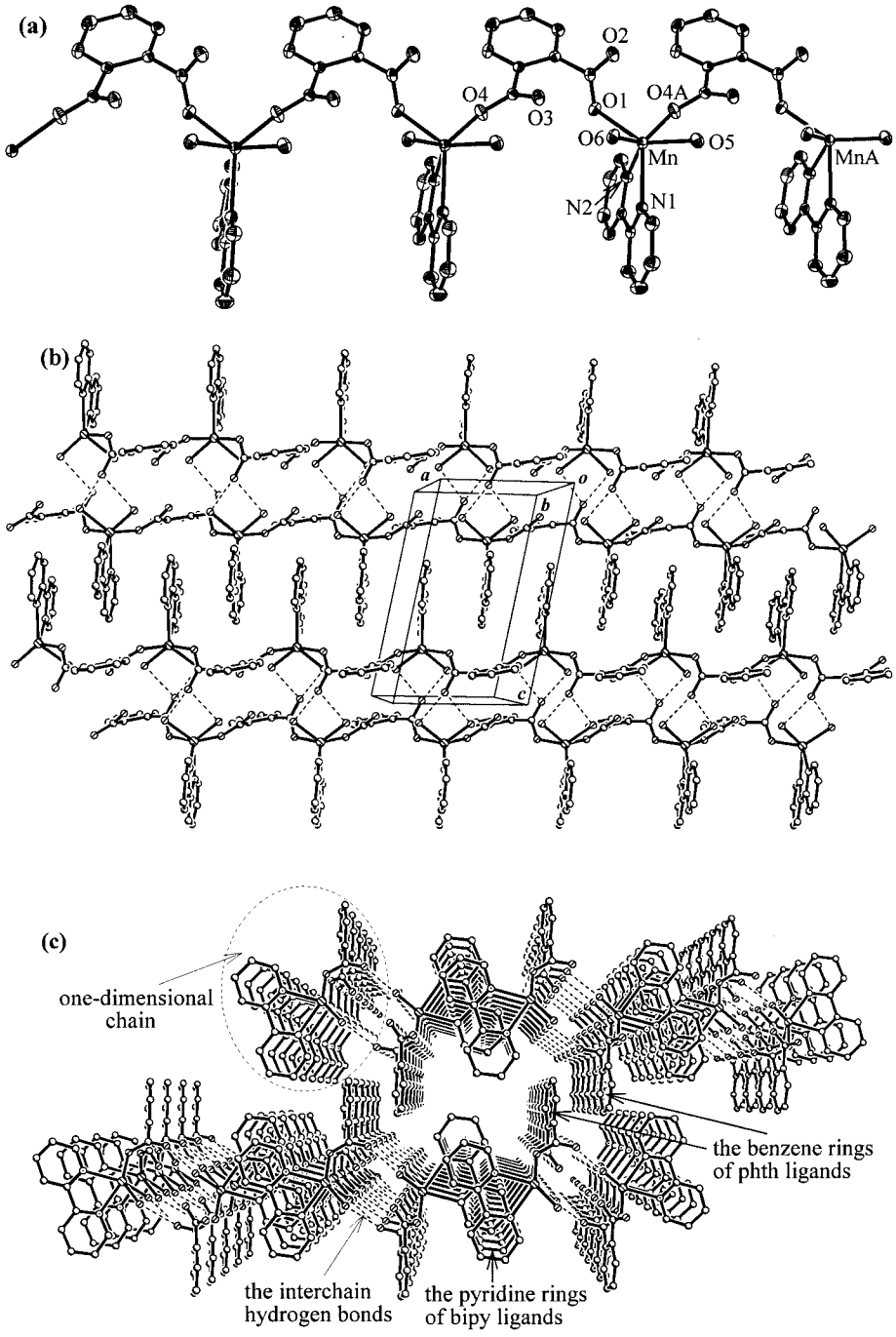

Figure 7. (a) The 1D chain structure of **6** (ellipsoids at 30% probability); (b) a view of the 2D supramolecular layer in **6**; (c) the packing diagram of **6**, showing the 3D supramolecular network sustained by complicated supramolecular contacts

that found in the known complex [Mn(phth)(phen)-$(H_2O)_2]_n$,[35] in which the phth dianion employs just one carboxylate group to bridge two Mn atoms, with the other free. Interestingly, in compound **6** two neighboring chains connect to each other by a hydrogen-bonding interactions [O5···O2# 2.884 Å; O6···O2# 2.712 Å; #: $-x + 1, -y, -z$] to form a set of 1D hydrogen-bonded double-chains with the bipy ligands growing outwards at both sides of the double-chain (Figure 7b). Meanwhile, the adjacent two sets of the double-chains are correlated through π-π stacking interactions between the bipy ligands, with face-to-face distances of about 3.512 Å and 3.535 Å (Figure 7b) to construct a 2D layer, which is further packed into a 3D supramolecular network (Figure 7c) through inter-layer π-π stacking interactions between the benzene rings of the phth ligands with a face-to-face distance of about 3.450 Å.

Table 4. Selected bond lengths (Å) and angles (°) in **6** and **7**

Complex **6**			
Mn−O1	2.128(2)	O5−Mn−O6	83.37(8)
Mn−O4A[a]	2.135(2)	O1−Mn−N2	83.99(8)
Mn−O5	2.193(2)	O4A−Mn−N2	82.81(9)
Mn−O6	2.285(2)	O5−Mn−N2	131.01(9)
Mn−N2	2.289(2)	O6−Mn−N2	132.14(9)
Mn−N1	2.312(2)	O1−Mn−N1	126.47(9)
O1−Mn−O4A	86.99(9)	O4A−Mn−N1	132.12(9)
O1−Mn−O5	141.72(8)	O5−Mn−N1	85.62(8)
O4A−Mn−O5	83.57(8)	O6−Mn−N1	83.46(8)
O1−Mn−O6	80.82(8)	N2−Mn−N1	70.04(9)
O4A−Mn−O6	140.66(9)		
Complex **7**			
Mn−O1	2.132(3)	O3A−Mn−O3	178.6(2)
Mn−O3	2.166(3)	O1−Mn−N2B	93.30(9)
Mn−N2B[a]	2.330(5)	O3−Mn−N2B	89.32(10)
Mn−N1	2.377(5)	O1−Mn−N1	86.70(9)
O1−Mn−O1A[a]	173.40(18)	O3−Mn−N1	90.68(10)
O1−Mn−O3A	86.32(12)	N2B−Mn−N1	180.000(1)
O1−Mn−O3	93.76(12)		

[a] Symmetry codes: (**6**) A: $x - 1, y, z$; (**7**) A: $-x + 1/2, -y + 3/2, z$; B: $x, -y + 3/2, z + 1/2$.

In the structure of **7**, as shown in Figure 8, the Mn atom is in a slightly distorted octahedral geometry (Table 4), being *trans*-coordinated by two N atoms [Mn−N1 = 2.377(5) Å, Mn−N2B = 2.330(5) Å] of μ-pyz ligands, two O atoms [Mn−O3 = 2.166(3) Å] of water molecules and two O atoms [Mn−O1 = 2.132(3) Å] from phth ligands. The phth ligand, in a coordination mode similar to that found in **6**, is coordinated to two Mn atoms through two O atoms from two carboxylate groups, resulting in a 1D $[Mn(phth)]_n$ chain in the *a* direction. The μ-pyz ligands link adjacent $[Mn(phth)]_n$ chains to generate an infinite 2D layer consisting of rectangular grids with dimensions of 7.511 × 7.630 Å measured through the μ-phth ligands and μ-pyz ligands, respectively. The adjacent layers parallel to each other are further inter-connected into a stacked multi-layer 3D supramolecular network through an inter-layer hydrogen bond between the water ligand and the carboxylate O atom [O3···O2# 2.762 Å; #: $-x, y + 1/2, -z + 1/2$] (Figure 9). Compound **7** is the first example of a Mn complex with both carboxylate and pyrazine ligands.

Magnetic Properties

The variable-temperature (5−300 K) magnetic behaviors of complexes **1** and **6**, and **3** and **4**, in the form of μ_{eff} vs. T plots are shown in Figure 10 and 11, respectively.

As shown in these figures, at room temperature the experimental effective magnetic moments (μ_{eff}) of 5.94 and 6.04 μ_B of **1** and **6**, respectively, are close to the value (5.92 μ_B) expected for one isolated Mn ion ($S = 5/2$); while the μ_{eff} value (11.75 μ_B or so) of **3** and **4** per Mn_4 unit is also close

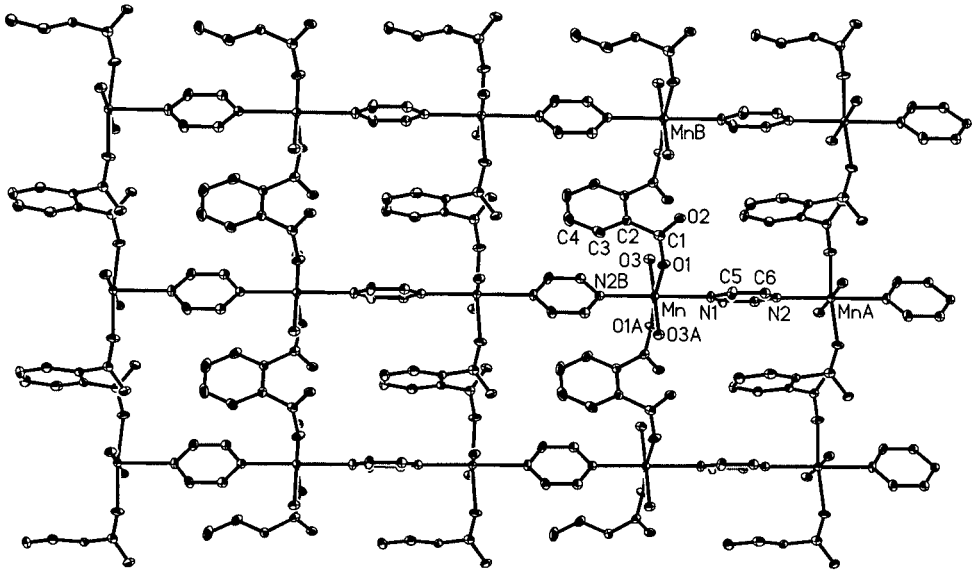

Figure 8. The 2D layer structure of **7** (ellipsoids at 30% probability)

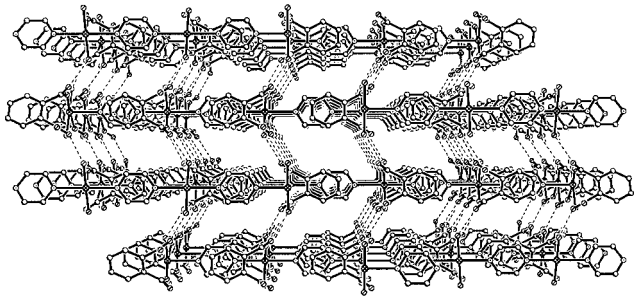

Figure 9. The packing diagram of **7**, showing the multi-layer-stacked 3D hydrogen-bonded network; the inter-layer hydrogen bonds are indicated by dotted lines

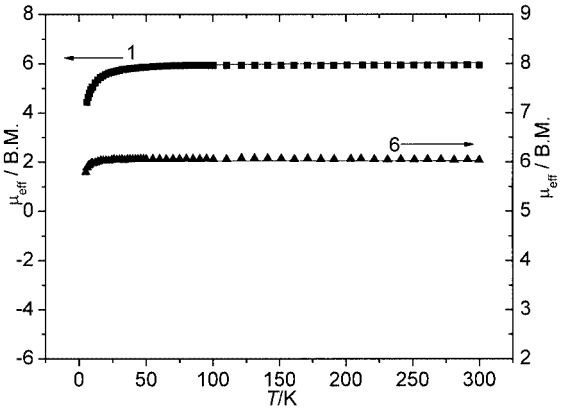

Figure 10. Effective magnetic moment (μ_{eff}) as function of temperature for **1** (■) and **6** (▲); the solid lines represent the calculated values

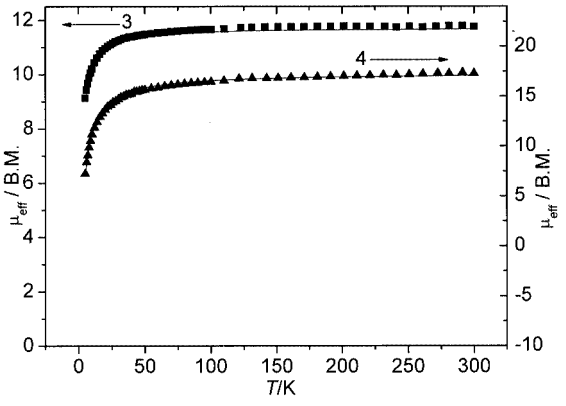

Figure 11. Effective magnetic moment (μ_{eff}) as function of temperature for **3** (■) and **4** (▲); the solid lines represent the calculated values

to the expected value of 11.83 μ_B. As the temperature is lowered to 75 K or lower, the μ_{eff} values remain essentially constant and then decrease gradually, indicative of an overall antiferromagnetic coupling between Mn^{2+} ions for these complexes. A dinuclear Heisenberg model ($H = -JS_1 \cdot S_2$) and a uniform chain model[50] ($\boldsymbol{H} = -2J \cdot \Sigma \boldsymbol{S}_i \cdot \boldsymbol{S}_{i+1}$) were used to fit the experimental data of **1** and **6**, respectively. The best-fit parameters over the full temperature range are as follows: $J = -0.34(4)$ cm^{-1}, $g = 2.04(9)$ and $R = 1.91 \times 10^{-4}$ for **1**; $J = -0.01(4)$ cm^{-1}, $g = 2.03$ and $R = 3.33 \times 10^{-4}$ for **6**, with the agreement factor, R, defined as $\Sigma[(\chi_M T)_{calcd.} - (\chi_M T)_{obsd.}]^2/[\Sigma(\chi_M T)_{obsd.}]^2$.

In either rhombic Mn_4 entity of **3** or rectangular Mn_4 entity of **4**, there are two possible exchange pathways: one through the μ-OCO bridge, and the other through both carboxylate moieties involving the benzene ring (Mn1−O4−C32−C31−C26−C25−O2−Mn2 in **3** and the similar path in **4**). The latter transmission of the coupling can be considered very small and negligible, therefore dinuclear and tetranuclear rectangular Heisenberg models were used for **3** [$H = -J(S_1 \cdot S_2)$] and **4** [$H = -2J(S_1 \cdot S_2 + S_2 \cdot S_3 + S_3 \cdot S_4 + S_4 \cdot S_1)$] to fit their experimental data, based on the consideration that all the coupling parameters (J) between adjacent pairs of Mn^{2+} ions are equal. The best-fit parameters over the full temperature range are as follows: $J = -1.09$ cm^{-1}, $g = 1.97$ and $R = 6.59 \times 10^{-4}$ for **3**; $J = -0.26$ cm^{-1}, $g = 2.00$ and $R = 2.25 \times 10^{-4}$ for **4**.

For complex **3**, the superexchange constant J (-1.09 cm^{-1}), corresponding to the coupling interaction between Mn1 and Mn1A doubly bridged by carboxylates of phth ligands (Figure 3), is similar to those previously reported between Mn^{2+} ions with a similar bridging network (J between -0.96 and -1.84 cm^{-1}),[9,12,51−54] and indicates the presence of a weak antiferromagnetic coupling through the short pathway of the carboxylate bridge of phth. A larger J value than that found in compound **1** [$-0.34(4)$ cm^{-1}] agrees well with the shorter metal−metal separation of 4.170 Å in **3** (4.786 Å in **1**).

For complex **4**, the small value of the superexchange constant ($J = -0.26$ cm^{-1}), corresponding to the coupling interaction transmitted by a single *syn-anti* carboxylate of a phth ligand (Figure 5), can be considered as normal, taking into account the nature of the bridging carboxylate. The exchange coupling through the carboxylato moiety is largely determined by the conformation of the bridge between two interacting metal centers.[55] Of three most common carboxylato bridging conformations (*syn-syn*, *anti-anti* and *syn-anti*), the *syn-anti* carboxylato bridge induces a much smaller J value than the other two types of conformations because of the expanded metallic core and the mismatch in the orientation of magnetic orbitals related to the high asymmetry of the *syn-anti* bridging network.[56] The non-planarity of the Mn−OCO−Mn bridging network accounts for the small value of the magnetic coupling interactions.

Conclusion

The phthalate-Mn^{2+}-diimine(bipy/phen/pyz) reaction system has been explored, and the ability of phthalate to act as a bridging ligand has been confirmed by synthesizing a new series of compounds (**1**−**7**), which show a variety of nuclearities and dimensionalities. Two singly deprotonated Hphth ligands bridging two Mn atoms in both dinuclear compounds **1** and **2** in a *syn-anti* conformation give the largest $Mn^{2+} \cdots Mn^{2+}$ distance among analogous dinuclear Mn^{2+} complexes. The coordination mode shown in

Scheme 1b is found for the first time in metal phthalate complexes, and compound **3** represents a novel structural type of Mn_4 clusters, with unique μ_3-phthalates supporting a rhombic Mn_4 unit. Two new tetranuclear compounds **4** and **5** crystallise as different salts, with the four Mn atoms located at the four corners of an approximate rectangle bridged by four *syn-anti* carboxylates of two phth ligands. The novel 2D layer network of compound **7** is reasonably formed from the novel 1D singly phth-bridged chain of compound **6** when the secondary bridging μ-pyz ligand is used in place of the end-capping bipy ligand. Although the Mn-acetate/benzoate-diimine(bipy/phen) system has given several compounds before, the new series of compounds reported in this work provides an important addition to the family of still poorly developed manganese dicarboxylate complexes, especially those in a discrete form.

Variable-temperature magnetic susceptibility measurements of compounds **1**, **3**, **4** and **6** reveal weak antiferromagnetic coupling interactions in all cases mediated through either the carboxylate group of the phth ligand or the whole extended phth ligand. The result indicates that, although magnetic interactions transmitted through the phth, as expected, are weak, the magnitude and nature of the coupling interactions can be influenced by various factors, such as the metal−metal separation, the carboxylate bridging modes and the degree of coplanarity of the bridging network.

Experimental Section

General Remarks: All chemicals were of reagent grade and used as received. Elemental analyses were performed with a Vario EL III CHNOS element analyzer. IR spectra of KBr pellets (4000−400 cm^{-1}) were recorded with a Magna-75 FT-IR spectrophotometer. The variable-temperature susceptibility (5−300 K) was measured with a model CF-1 superconducting extraction sample magnetometer in a 10 kG applied field with the crystalline sample kept in a capsule for weighing. Diamagnetic corrections were estimated with Pascal's table.[57]

$[Mn_2(Hphth)_2(phen)_4](Hphth)_2·2H_2O$ (1): A solution of 1,10-phenanthroline (phen) (0.40 g, 2 mmol) in EtOH (10 mL) was slowly addded with continuous stirring to an aqueous solution (20 mL) containing $Mn(OAC)_2·4H_2O$ (0.25 g, 1 mmol), phthalic acid (H_2phth; 0.17 g, 1 mmol) and KOH (0.056 g. 1 mmol). The mixture was stirred for five minutes at room temperature, then filtered. The filtrate was left to stand at room temperature for one week or so to deposit yellow crystals of **1** in 47% yield (0.72 g). $C_{80}H_{56}Mn_2N_8O_{18}$ (1527.2): calcd. C 62.91, H 3.70, N 7.34; found C 62.88, H 3.74, N 7.39. IR (KBr): $\tilde{\nu}$ = 3438 (m), 3068 (m), 1689 (s), 1591 (vs), 1558 (m), 1516 (s), 1497 (m), 1448 (m), 1425 (s), 1410 (vs), 1356 (m), 1342 (m), 1284 (m), 1254 (m), 1221 (m), 1159 (m), 1140 (m), 1101 (m), 1043 (m), 964 (m), 897 (w), 866 (m), 852 (s), 845 (s), 810 (m), 789 (m), 771 (m) 758 (m), 739 (m), 729 (vs), 681 (w), 638 (m), 627 (m), 584 (m), 555 (w), 434 (w), 420 (m) cm^{-1}.

$[Mn_2(Hphth)_2(phen)_4](ClO_4)_2·2H_2O$ (2): Compound **2** was prepared using a procedure similar to that used for preparing **1**, except that $Mn(ClO_4)_2·6H_2O$ was used as the starting Mn^{2+} source. Yellow crystals of **2** were obtained in 33% yield (0.46 g). $C_{64}H_{46}Cl_2Mn_2N_8O_{18}$ (1395.9): calcd. C 55.07, H 3.32, N 8.03; found C 55.02, H 3.34, N 8.07. IR (KBr): $\tilde{\nu}$ = 3427 (br. m), 3088 (m), 1701 (s), 1587 (vs), 1544 (m), 1493 (m), 1441 (m), 1411 (vs), 1367 (m),1348 (w), 1258 (w), 1142 (m), 1089 (s), 1043 (m), 1011 (m), 841 (m), 817 (m), 769 (m), 728 (s), 661 (m), 628 (m), 561 (m), 452 (w), 419 (m) cm^{-1}.

$[Mn_4(phth)_4(phen)_4(H_2O)_4]·2EtOH$ (3) and $\{[Mn_4(phth)_2(phen)_8](PF_6)_4\}_2$ (4): Compounds **3** and **4** were obtained from a one-pot synthetic procedure: A yellow suspension containing H_2phth (0.68 g, 4 mmol), KOH (0.46 g, 8 mmol), $Mn(OAc)_2·4H_2O$ (1.00 g, 4 mmol), phen (0.80 g, 4 mmol) and $(NMe_4)PF_6·6H_2O$ (1.31 g, 4 mmol) in H_2O/EtOH (1:1, 40 mL) was heated to reflux in a 50 mL round-bottomed flask for 10 days, during which time the yellow suspension turned tclear, and a large yellow cube-like crystal of **3** formed. Heating at lower temperature than before for an additional 2 d, during which time many soft and flimsy sheet crystals of **4** were deposited on the surface of the crystal of **3**. Crystals of **3** and **4** were mechanically collected in 27% yield (0.48 g) and 19% yield (0.49 g), respectively (based on Mn).

3: $C_{84}H_{68}Mn_4N_8O_{22}$ (1761.2): calcd. C 57.29, H 3.89, N 6.36; found C 57.33, H 3.81, N 6.43. IR (KBr): $\tilde{\nu}$ = 3450 (s), 3331 (br. s), 3062 (m), 1626 (s), 1547 (vs), 1516 (vs), 1495 (m), 1448 (m), 1423 (vs), 1402 (vs), 1342 (m), 1292 (w), 1219 (w), 1142 (w), 1101 (m), 1090 (m), 1043 (m), 995 (w), 941 (w), 864 (m), 850 (s), 812 (w), 781 (m), 758 (m), 729 (s), 702 (m), 648 (m), 636 (w), 592 (w), 557 (w), 451 (m), 420 (m) cm^{-1}.

4: $C_{224}H_{144}F_{48}Mn_8N_{32}O_{16}P_8$ (5139.0): calcd. C 52.35, H 2.82, N 8.72; found C 52.41, H 2.90, N 8.69. IR (KBr): $\tilde{\nu}$ = 3421 (w), 3079 (w), 1608 (s), 1591 (vs), 1566 (vs), 1497 (m), 1444 (m), 1425 (vs), 1407 (w), 1342 (m), 1317 (w), 1301 (w), 1223 (m), 1145 (m), 1103 (m), 1090 (w), 1049 (w), 953 (w), 841 (vs), 773 (w), 729 (s), 773 (m), 729 (s), 698 (w), 649 (w), 640 (w), 559 (s), 472 (w), 445 (w), 420 (m) cm^{-1}.

$[Mn_4(phth)_2(bipy)_8](ClO_4)_4·2EtOH$ (5): Compound **5** was obtained using a procedure similar to that used for preparing **2**, except that 2,2′-bipyridine (bipy) was used as the starting diimine species. Large yellow crystals of **5** were obtained in 56.5% yield (0.32 g). $C_{100}H_{84}Cl_4Mn_4N_{16}O_{26}$ (2287.4): calcd. C 52.51, H 3.70, N 9.80; found C 52.49, H 3.75, N 9.84. IR (KBr): $\tilde{\nu}$ = 3481 (br. m), 3070 (m), 1606 (m), 1593 (vs), 1564 (vs), 1489 (w), 1473 (m), 1439 (vs), 1417 (m), 1400 (m),1315 (w), 1248 (w), 1176 (w), 1142 (m), 1090 (vs), 1043 (w), 1014 (s), 862 (w), 833 (w), 814 (w), 764 (s), 739 (s), 727 (m), 696 (w), 652 (m), 623 (s), 558 (w), 567 (w), 449 (w), 415 (m) cm^{-1}.

$[Mn(phth)(bipy)(H_2O)_2]_n$ (6): A mixture containing $Mn(OAc)_2·4H_2O$ (0.50 g, 2 mmol), H_2phth (0.34 g, 2 mmol), KOH (0.22 g, 4 mmol) and bipy (0.31 g, 2 mmol) in EtOH/H_2O (1:5, 60 mL) was heated to reflux for 4 hours in a 100 mL round-bottomed flask, then filtered. The filtrate was left undisturbed at 4 °C for one month or so, resulting in the deposition of light-yellow crystals of **6** in 21.3% yield (0.18 g). $C_{18}H_{16}MnN_2O_6$ (411.27): calcd. C 52.56, H 3.92, N 6.81; found C 52.61, H 3.96, N 6.84. IR (KBr): $\tilde{\nu}$ = 3450 (br. m), 1603 (s), 1581 (vs), 1494 (m), 1414 (vs), 1389 (m), 1233 (m), 1250 (m), 1239 (m), 1111 (w), 884 (w), 826 (m), 756 (s), 690 (m), 645 (m), 589 (w), 525 (m), 411 (m) cm^{-1}.

$[Mn(phth)(pyz)(H_2O)_2]_n$ (7): A suspension containing $Mn(OAc)_2·4H_2O$ (0.50 g, 2 mmol), H_2phth (0.34 g, 2 mmol), KOH (0.22 g, 4 mmol) and pyrazine (pyz; 0.16 g, 2 mmol) in MeOH/H_2O (1:4, 20 mL) was heated at 140 °C for 4 days under autogenous pressure in a 25 mL sealed Teflon-lined stainless-steel vessel, then allowed to cool to room temperature, to give pale-yellow crystals

Table 5. Crystallographic data for complexes **1**−**3**

	1	**2**	**3**
Empirical formula	$C_{80}H_{56}Mn_2N_8O_{18}$	$C_{64}H_{46}Cl_2Mn_2N_8O_{18}$	$C_{84}H_{68}Mn_4N_8O_{22}$
Molecular mass	1527.21	1395.87	1761.22
Space group	$P\bar{1}$	$P\bar{1}$	$P\bar{1}$
a (Å)	11.8388(2)	10.6882(3)	12.3449(2)
b (Å)	12.26390(10)	12.1634(3)	12.5268(2)
c (Å)	13.6053(2)	13.6195(3)	14.77880(10)
α (°)	110.6900(10)	108.48	115.0320(10)
β (°)	97.6450(10)	96.3030(10)	93.6410(10)
γ (°)	93.5350(10)	105.0000(10)	109.1450(10)
V (Å^3)	1818.91(4)	1586.10(7)	1900.82(5)
Z	1	1	1
T (°C)	20	20	20
λ (Mo-K_α) (Å)	0.71037	0.71037	0.71037
ρ_{calcd}.(g·cm^{-3})	1.394	1.461	1.539
μ (mm^{-1})	0.425	0.561	0.734
R[a]	0.0421	0.0496	0.0442
wR[b]	0.1127	0.1246	0.0948

[a] $R = \Sigma||F_o| - |F_c||/\Sigma|F_o|$. [b] $wR = [\Sigma w(|F_o| - |F_c|)^2/\Sigma wF_o^2]^{1/2}$.

Table 6. Crystallographic data for complexes **4**−**7**

	4	**5**	**6**	**7**
Empirical formula	$C_{224}H_{144}F_{48}Mn_8N_{32}O_{16}P_8$	$C_{100}H_{84}Cl_4Mn_4N_{16}O_{26}$	$C_{18}H_{16}MnN_2O_6$	$C_{12}H_{12}MnN_2O_6$
Molecular mass	5138.99	2287.39	411.27	335.18
Space group	$P\bar{1}$	$P\bar{1}$	$P\bar{1}$	$Pccn$
a (Å)	14.52200(10)	14.2703(4)	7.1312(5)	7.6296(11)
b (Å)	18.6579(3)	14.3887(4)	10.1622(8)	11.4509(14)
c (Å)	21.2235(3)	15.3922(4)	11.9270(9)	15.021(2)
α (°)	83.7010(10)	88.5840(10)	88.758(2)	90
β (°)	83.4490(10)	63.2820(10)	79.0820(10)	90
γ (°)	81.4470(10)	66.6120(10)	89.269(2)	90
V (Å^3)	5624.19(13)	2545.13(12)	848.46(11)	1312.3(3)
Z	1	1	2	4
T (°C)	20	20	20	20
λ (Mo-K_α) (Å)	0.71037	0.71037	0.71037	0.71037
ρ_{calcd}.(g·cm^{-3})	1.517	1.492	1.610	1.696
μ (mm^{-1})	0.600	0.674	0.818	1.036
R[a]	0.0796	0.0595	0.0441	0.0455
wR[b]	0.1759	0.1445	0.1089	0.0885

[a] $R = \Sigma||F_o| - |F_c||/\Sigma|F_o|$. [b] $wR = [\Sigma w(|F_o| - |F_c|)^2/\Sigma wF_o^2]^{1/2}$.

of **7** in 12.4% yield (0.08 g). $C_{12}H_{12}MnN_2O_6$ (335.18): calcd. C 43.00, H 3.61, N 8.36; found C 43.03, H 3.67, N 8.33. IR (KBr): $\tilde{\nu}$ = 3405 (m), 3218 (br. m), 1608 (s), 1547 (vs), 1486 (m), 1419 (vs), 1329 (m), 1088 (m), 1007 (m), 831 (m), 800 (w), 764 (s), 731 (w), 696 (w), 637 (m), 528 (m), 420 (m) cm^{-1}.

X-ray Crystallographic Study: Intensity data for complexes **1**−**7** were collected at 293 K with a Siemens SMART CCD diffractometer equipped with graphite-monochromated Mo-K_α radiation (λ = 0.71073 Å). An empirical absorption correction was applied by using the SADABS program, and the structures were solved by direct methods and refined on F^2 by a full-matrix least-squares procedure with the SHELXTL-97 program package.[58] Non-hydrogen atoms were refined anisotropically, with the exceptions of F22, F23 and F24 in one of the PF_6^- ions in **4**, which were refined isotropically. Hydrogen atoms were introduced geometrically except for those on the water molecules and the solvate ethanol molecules, which were located from the difference Fourier syntheses and refined isotropically. Crystallographic data of **1**−**7** are outlined in Table 5 and 6.

CCDC-231921 to -231927 (for **1**−**7**, respectively) contain the supplementary crystallographic data for this paper. These data can be obtained free of charge at www.ccdc.cam.ac.uk/conts/retrieving.html [or from the Cambridge Crystallographic Data Centre, 12 Union Road, Cambridge CB2 1EZ, UK; Fax: +44-1223-336033; E-mail: deposit@ccdc.cam.ac.uk].

Acknowledgments

This work was supported by NNSFC (No. 30170229), the 973 Project of China (G1998010100, G001CB108906), and the State Expert Project of Key Basic Research (2001CCA02500).

[1] J. S. Miller, A. J. Epstein, *Angew. Chem. Int. Ed. Engl.* **1994**, *33*, 385−415.
[2] C. P. Landee, M. Melville, J. S. Miller, *Magnetic Molecular Ma-*

terials (Eds.: D. Gatteschi, O. Kahn, J. S. Miller, F. Palacio), Kluwer, Dordrecht, The Netherlands, **1991**.
[3] C. T. Chen, K. S. Suslick, *Coord. Chem. Rev.* **1993**, *128*, 293−322.
[4] K. Wieghardt, *Angew. Chem. Int. Ed. Engl.* **1989**, *28*, 1153−1172.
[5] N. A. Law, M. T. Caudle, V. L. Pecoraro, *Adv. Inorg. Chem.* **1999**, *46*, 305−440.
[6] L. Que Jr., A. True, *Prog. Inorg. Chem.* **1990**, *38*, 97−200.
[7] E. G. Bakalbassis, A. P. Bozopoulos, J. Mrozinski, P. J. Rentzeperis, C. A. Tripis, *Inorg. Chem.* **1988**, *27*, 529−532.
[8] P. Chaudhuri, K. Oder, K. Weighardt, S. Ghering, W. Haase, B. Nuber, J. Weiss, *J. Am. Chem. Soc.* **1988**, *110*, 3657−3658.
[9] J. Cano, G. Demunno, J. Sanz, R. Ruiz, F. Lloret, J. Faus, M. Julve, *J. Chem. Soc., Dalton Trans.* **1994**, 3465−3469, and references cited therein.
[10] K. S. Bürger, P. Chaudhuri, K. Wieghardt, B. Nuber, *Chem. Eur. J.* **1995**, *1*, 583−593.
[11] J. Cano, G. D. Munno, J. L. Sanz, R. Ruiz, J. Faus, F. Lloret, M. Julve, A. Caneschi, *J. Chem. Soc., Dalton Trans.* **1997**, 1915−1523, and references cited therein.
[12] C. S. Hong, Y. Do, *Inorg. Chem.* **1997**, *36*, 5684−5685.
[13] D.-F. Xiang, X.-S. Tan, Q.-W. Hang, W.-X. Tang, B.-M. Wu, T. C. W. Mak, *Inorg. Chim. Acta* **1998**, *277*, 21−25.
[14] L. Deakin, A. M. Arif, J. S. Miller, *Inorg. Chem.* **1999**, *38*, 5072−5077.
[15] E. G. Bakalbassis, P. Bergerat, O. Kahn, S. Jeannin, Y. Jeannin, Y. Dromzee, M. Guillot, *Inorg. Chem.* **1992**, *31*, 625−631.
[16] D.-F. Sun, R. Cao, Y.-C. Liang, Q. Shi, W.-P. Su, M.-C. Hong, *J. Chem. Soc., Dalton Trans.* **2001**, 2335−2340.
[17] L.-C. Li, D.-Z. Liao, Z.-H. Jiang, S.-P. Yan, *Inorg. Chem.* **2002**, *41*, 421−424.
[18] E. K. Shakhatreh, E. G. Bakalbassis, I. Brudgam, H. Hartl, J. Mrozinski, C. A. Tsipis, *Inorg. Chem.* **1991**, *30*, 2801−2806.
[19] A. Escuer, R. Vicente, F. A. Mautner, A. S. M. Goher, *Inorg. Chem.* **1997**, *36*, 1233−1236.
[20] E. G. Bakalbassis, D. G. Paschalidis, C. P. Raptopoulou, V. Tangoulis, *Inorg. Chem.* **1998**, *37*, 4735−4737.
[21] H.-X. Zhang, B.-S. Kang, A.-W. Xu, Z.-N. Chen, Z.-Y. Zhou, A. S. C. Chan, K.-B. Yu, C. Chen, *J. Chem. Soc., Dalton Trans.* **2001**, 2559−2566, and references cited therein.
[22] V. L. Pecoraro, *Manganese Redox Enzymes*, VCH Publishers, New York, **1992**.
[23] F. C. Wedler, *Manganese in Health and Disease* (Ed.: D. J. Klimis-Tavantzis), CRC Press, Inc., Ann Arbor, **1994**.
[24] S. V. Antonyuk, V. R. Melikadamyan, A. N. Popov, V. S. Lamzin, P. D. Hempstead, P. M. Harrison, P. J. Artymyuk, V. V. Barynin, *Crystallogr. Rep.* **2000**, *45*, 105−116.
[25] A. Willing, H. Follmann, G. Auling, *Eur. J. Biochem.* **1988**, *170*, 603−611.
[26] R. J. Debus, *Biochim. Biophys. Acta* **1992**, *1102*, 269−271.
[27] A. Zouni, H. T. Witt, J. Kern, P. Fromme, N. Krauß, W. Saenger, P. Orth, *Nature* **2001**, *409*, 739−743.
[28] G. B. Conyers, G. Wu, M. J. Bessman, A. S. Mildvan, *Biochemistry* **2000**, *39*, 2347−2354.
[29] G. Christou, *Acc. Chem. Res.* **1989**, *22*, 328−335, and references cited therein.
[30] M. W. Wemple, H. L. Tsai, S. Wang, J. P. Clude, W. E. Streib, J. C. Huffman, D. N. Hendrickson, G. Christou, *Inorg. Chem.* **1996**, *35*, 6437−6449.
[31] Z.-H. Jiang, S.-L. Ma, D.-Z. Liao, S.-P. Yan, G.-L. Wang, X.-K. Yao, R.-J. Wang, *J. Chem. Soc., Chem. Commun.* **1993**, 745−747.
[32] C. Canada-Vilalta, W. E. Streib, J. C. Huffman, T. A. O′Brien, E. R. Davidson, G. Christou, *Inorg. Chem.* **2004**, *43*, 101−115.
[33] C.-N. Chen, H.-P. Zhu, D.-G. Huang, T.-B. Wen, Q.-T. Liu, D.-Z. Liao, J.-Z. Cui, *Inorg. Chim. Acta* **2001**, *320*, 159−166.
[34] C.-B. Ma, C.-N. Chen, Q.-T. Liu, D.-Z. Liao, L.-C. Li, L.-C. Sun, *New J. Chem.* **2003**, *27*, 890−894.
[35] Y.-G. Zhang, J.-M. Li, M. Zhu, Q.-M. Wang, X.-T. Wu, *Chem. Lett.* **1998**, 1051−1052.
[36] R. Bermejo, M. Fondo, A. García-Deibe, A. M. González, A. Sousa, J. Sanmartín, C. A. McAuliffe, R. G. Pritchard, M. Watkinson, V. Lukov, *Inorg. Chim. Acta* **1999**, *293*, 210−217.
[37] C. Cañada-Vilalta, M. Pink, G. Christou, *Dalton Trans.* **2003**, 1121−1125.
[38] C.-B. Ma, W.-G. Wang, H.-P. Zhu, C.-N. Chen, Q.-T. Liu, *Inorg. Chem. Commun.* **2001**, *4*, 730−733.
[39] B. Albela, M. Corbella, J. Ribas, I. Castro, J. Sletten, H. Stoeckli-Evans, *Inorg. Chem.* **1998**, *37*, 788−798.
[40] R. L. Rardin, W. B. Tolman, S. J. Lippard, *New J. Chem.* **1991**, *15*, 417−430.
[41] G. Fernández, M. Corbella, J. Mahía, M. A. Maestro, *Eur. J. Inorg. Chem.* **2002**, 2502−2510.
[42] H. H. Thorp, *Inorg. Chem.* **1992**, *31*, 1585−1588.
[43] I. D. Brown, D. Altermatt, *Acta Crystallogr., Sect. B* **1985**, *41*, 244−247.
[44] G. Aromi, S. M. J. Aubin, M. A. Bolcar, G. Christou, H. J. Eppley, K. Folting, D. N. Hendrickson, J. C. Huffman, R. C. Squire, H.-L. Tsai, S. Wang, M. W. Wemple, *Polyhedron* **1998**, *17*, 3005−3020, and references cited therein.
[45] G. Aromi, M. W. Wemple, S. M. J. Aubin, K. Folting, D. N. Hendrickson, G. Christou, *J. Am. Chem. Soc.* **1998**, *120*, 5850−5851.
[46] R. J. Kulawiec, R. H. Crabtree, G. W. Brudvig, G. K. Schulte, G. K, *Inorg. Chem.* **1988**, *27*, 1309−1311.
[47] E. Libby, J. K. McCusker, E. A. Schmitt, K. Folting, D. N. Hendrickson, G. Christou, *Inorg. Chem.* **1991**, *30*, 3486−3495.
[48] S. Wang, K. Folting, W. E. Streib, E. A. Schmitt, J. K. McCusker, D. N. Hendrickson, G. Christou, *Angew. Chem. Int. Ed. Engl.* **1991**, *30*, 304−306.
[49] C. Gedye, C. Harding, V. Mckee, J. Nelson, J. Patterson, *J. Chem. Soc., Chem. Commun.* **1992**, 392−393.
[50] W. Hiller, J. Strahle, A. Datz, M. Hanack, W. E. Hatfield, L. W. TerHaar, P. Gutlich, *J. Am. Chem. Soc.* **1984**, *106*, 329−335.
[51] H. Oshio, E. Ino, I. Mogi, T. Ito, *Inorg. Chem.* **1993**, *32*, 5697−5703.
[52] B. Albela, M. Corbella, J. Ribas, I. Castro, J. Sletten, H. Stoeckli-Evans, *Inorg. Chem.* **1998**, *37*, 788−798.
[53] C. S. Hong, S.-K. Son, Y. S. Lee, M.-J. Jun, Y. Do, *Inorg. Chem.* **1999**, *38*, 5602−5610.
[54] P. S. Mukherjee, S. Konar, E. Zangrando, T. Mallah, J. Ribas, N. R. Chaudhuri, *Inorg. Chem.* **2003**, *42*, 2695−2703.
[55] O. Kahn, *Molecular Magnetism*, VCH, Weinheim (Germany), **1993**.
[56] C. Policar, F. Lambert, M. Cesario, I. Morgenstern-Badarau, *Eur. J. Inorg. Chem.* **1999**, 2201−2207, and references cited therein.
[57] P. Pascal, *Ann. Chim. Phys.* **1910**, *19*, 5−70.
[58] G. M. Sheldrick, *SHELXL-97*, University of Göttingen, **1997**.

Received February 28, 2004
Early View Article
Published Online June 23, 2004

